

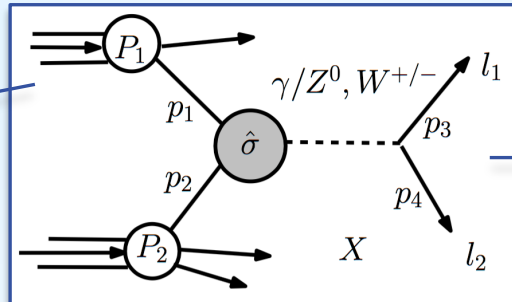
# Differential measurements of the Drell-Yan cross-sections

Ulla Blumenschein, QMUL London, on behalf of ATLAS



# Drell-Yan production

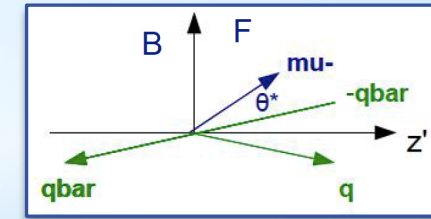
valence & sea PDF sensitivity through  $Z, W^+ \text{ and } W^- d\sigma/d\eta$



Weinberg angle:  $Z, \gamma$  mixing  
 $Z/\gamma^*$  interference  $\leftrightarrow M(l\bar{l})$   
 Different coupling to  $f_R, f_L$

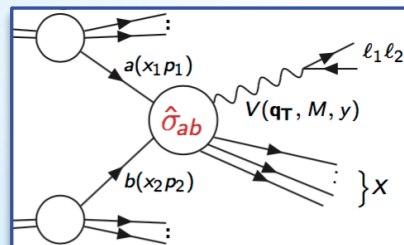
$$\begin{aligned} u\bar{d}, c\bar{s} \quad (u\bar{s}, c\bar{d}) &\rightarrow W^+, \\ d\bar{u}, s\bar{c} \quad (s\bar{u}, d\bar{c}) &\rightarrow W^-, \\ q\bar{q} &\rightarrow Z/\gamma^*, \end{aligned}$$

$$A_{FB} = \frac{\sigma_F - \sigma_B}{\sigma_F + \sigma_B}$$

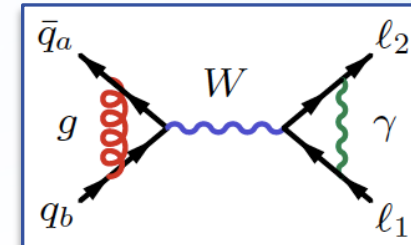


CS frame:  $\theta^* (l-q)$   
 $\rightarrow$  from  $y(l\bar{l}) \rightarrow$  dilution

hadronic activity:  
 NNLO ( $\rightarrow N^3NLO$ ) QCD

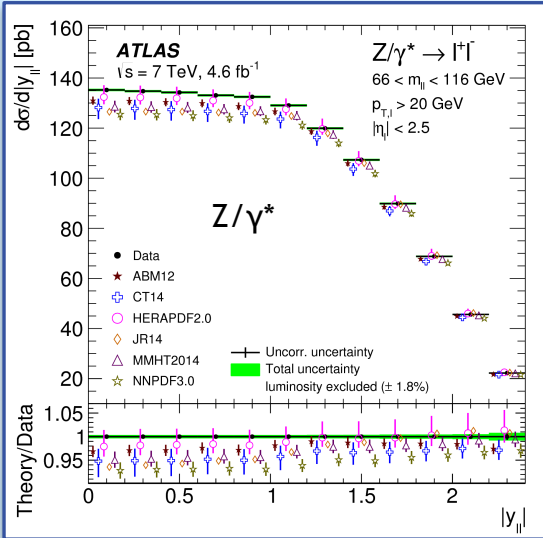


EWK & QCD corrections: mostly factorisable,  
 up to NNLO QCD + nNLO EWK, partly automated

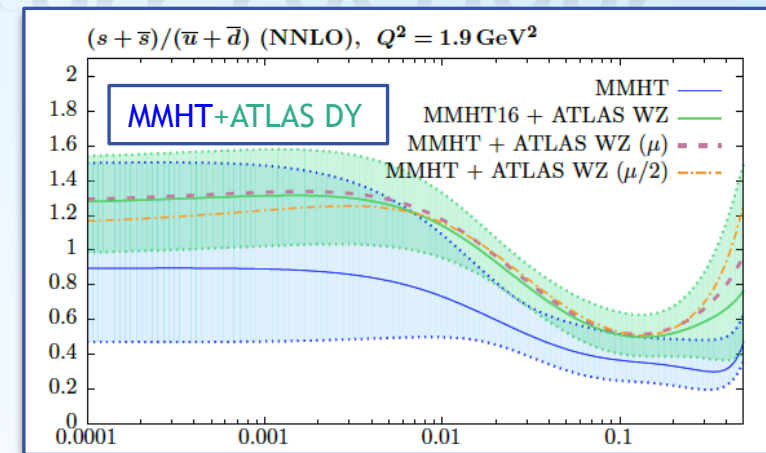


# 7TeV precise Z/W cross sections

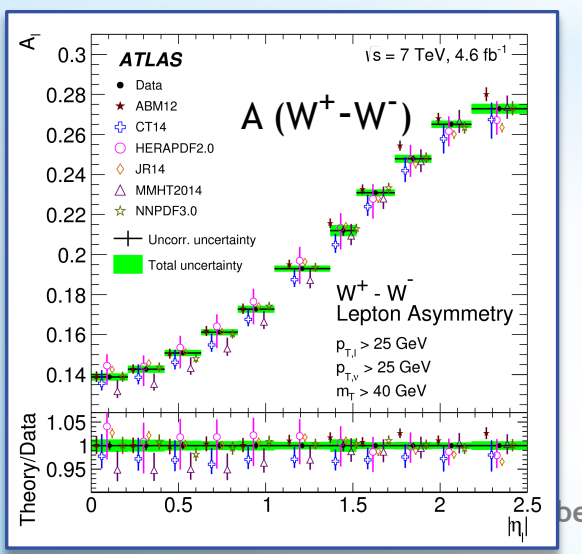
Eur. Phys. J. C 77 (2017) 367



Z/W inclusive and  $\eta$  differential cross sect.  
LHC 7-TeV data  
syst. uncertainty  $\approx 0.5\%$



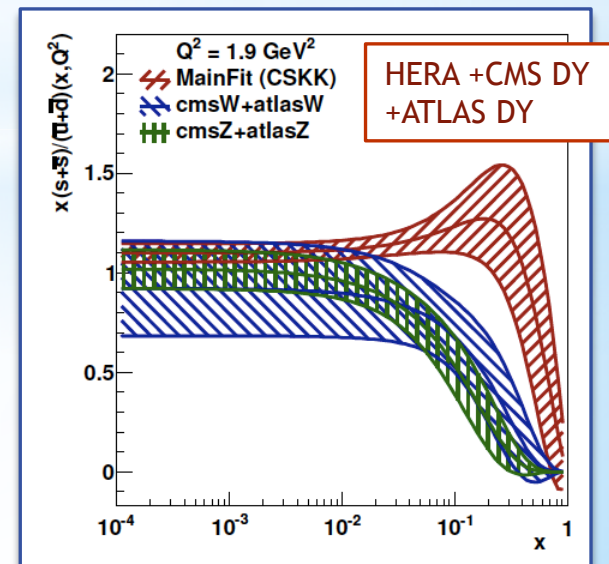
R.S. Thorne et al. arXiv:1708.00047



ATLAS data prefers unsuppressed strange sea.

Meanwhile included in Global fitters.

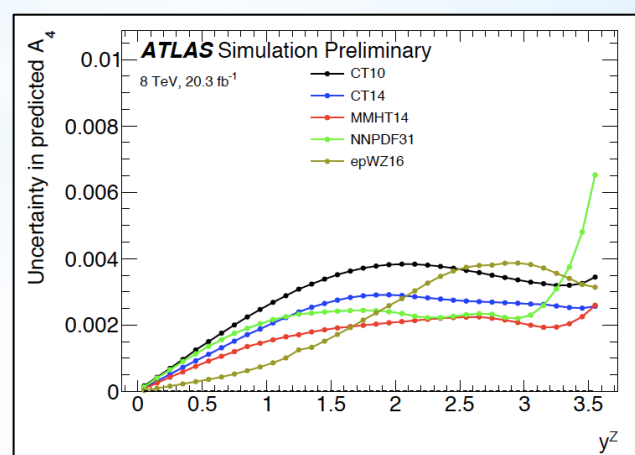
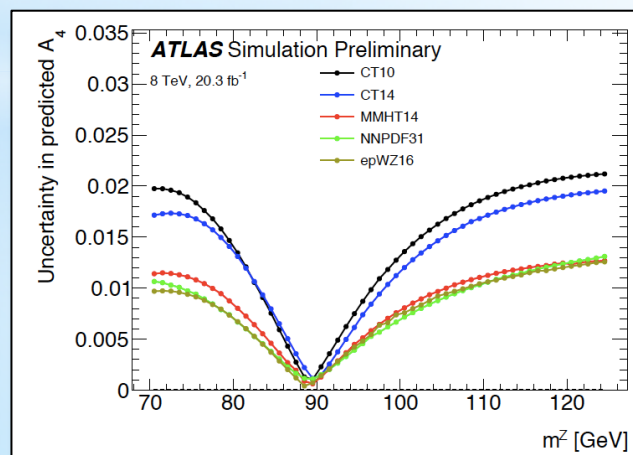
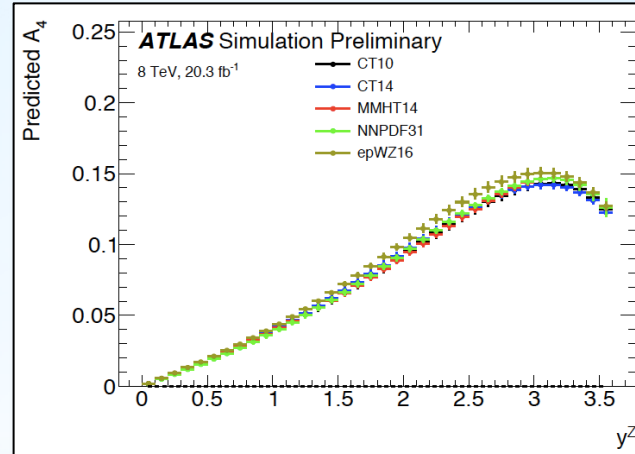
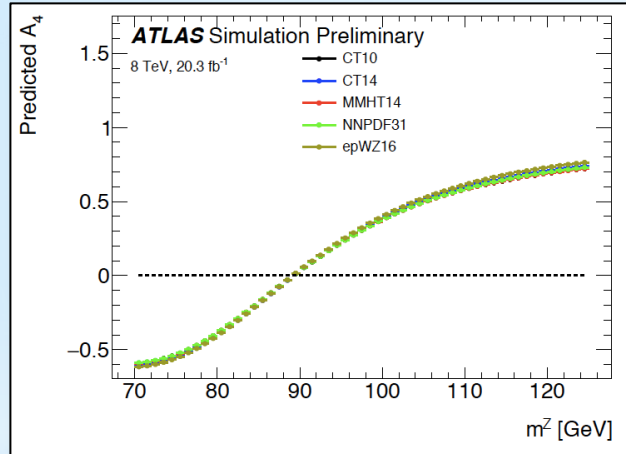
- Globally consistent but pulls in different direction from vs->lc DIS
- Prefers lower QCD scale
- Compatible with CMS DY dominates due to precision



A. Cooper-Sakar et al, arXiv:1803.00968

17/04/18

# PDF uncertainties on $A_{FB}$



$$A_{FB} \propto A_4$$

PDF sensitivity

- offpeak
- medium  $y$

$\sin^2\theta_W$  sensitivity:

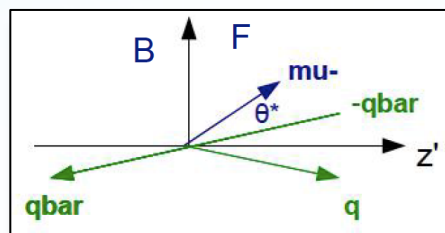
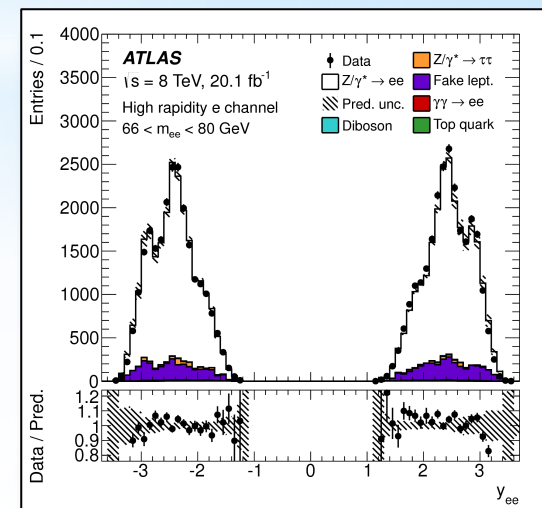
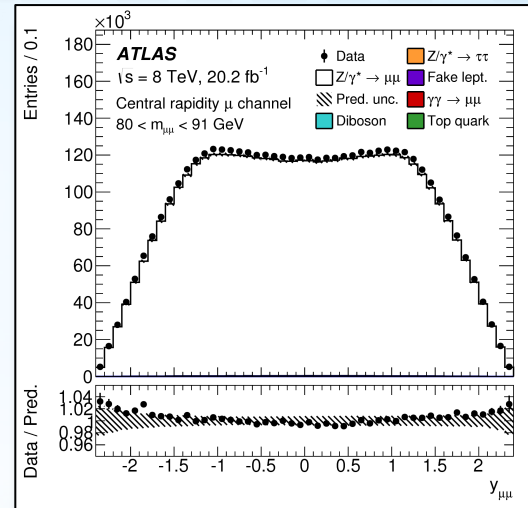
- slope at peak
- large  $y$

-> reduce PDF uncertainty by combined fit of  $\sin^2\theta_W$  and PDF

ATL-PHYS-PUB-2018-004

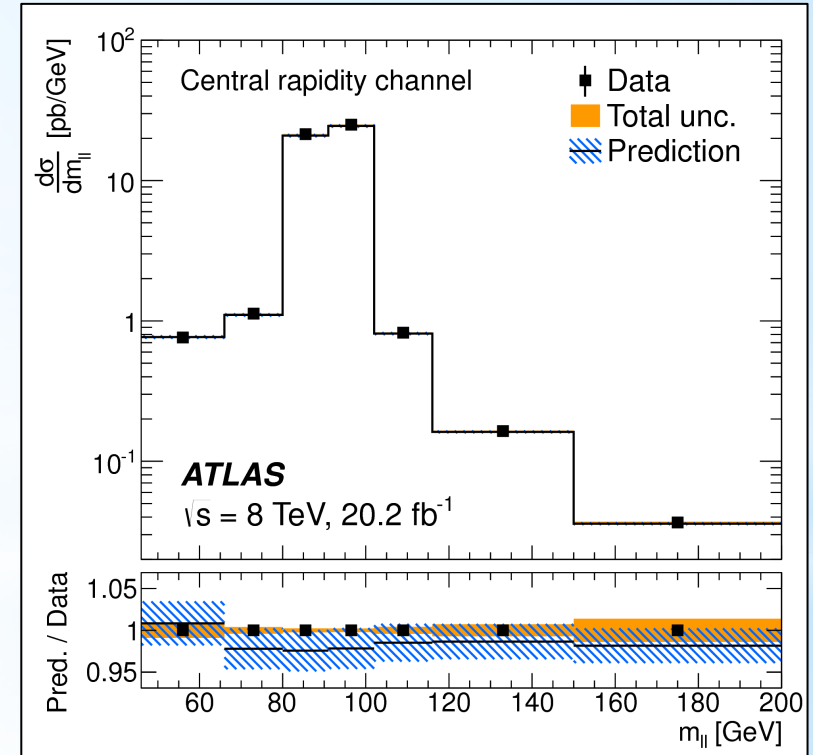
# Unfolded 3D DY cross sect.

- ATLAS, 8TeV data (2012)
- 3D cross section:
  - $m(l\bar{l})$ ,  $y(l\bar{l})$ ,  $\cos\theta^*$
  - Central electrons and muons ( $\eta < 2.5$ ) & Forward electrons ( $2.5 < \eta < 3.5$ )
  - 505 bins Central+Central
  - 150 bins Central+Forward
- Precision
  - Stat: 0.5% at peak
  - Exp: 0.5% at peak
  - Lumi: 1.9%
- Plan simultaneous constraint on  $\sin^2\theta_W$  & PDF



# Unfolded 3D DY cross sect.

- ❑ ATLAS, 8TeV data (2012)
- ❑ 3D cross section:
  - ❑  $m(l\bar{l})$ ,  $y(l\bar{l})$ ,  $\cos\theta^*$
  - ❑ Central electrons and muons ( $\eta < 2.5$ ) & Forward electrons ( $2.5 < \eta < 3.5$ )
  - ❑ 505 bins Central+Central
  - ❑ 150 bins Central+Forward
- ❑ Precision
  - ❑ Stat: 0.5% at peak
  - ❑ Exp: 0.5% at peak
  - ❑ Lumi: 1.9%
- ➔ Plan simultaneous constraint on  $\sin^2\theta_W$  & PDF

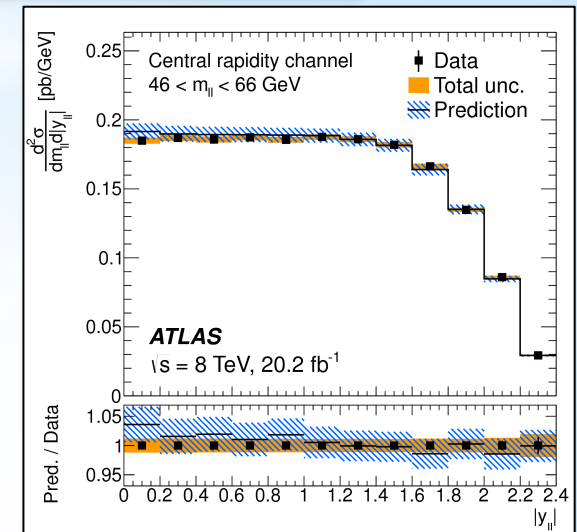
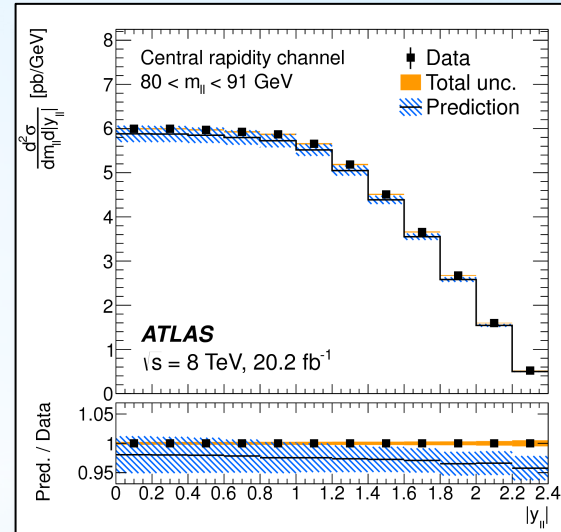


Good agreement with Powheg+Py8 with CT10,  $m(l\bar{l})$  dependent NNLO QCD + NLO EWK k-factor (FEWZ) and  $pT(l\bar{l})$  and  $y(l\bar{l})$  dependent angular coefficient corrections at NNLO (DYNNLO)

# Unfolded 3D DY cross sect.

- ❑ ATLAS, 8TeV data (2012)
- ❑ 3D cross section:
  - ❑  $m(l\bar{l})$ ,  $y(l\bar{l})$ ,  $\cos\theta^*$
  - ❑ Central electrons and muons ( $\eta < 2.5$ ) & Forward electrons ( $2.5 < \eta < 3.5$ )
  - ❑ 505 bins Central+Central
  - ❑ 150 bins Central+Forward
- ❑ Precision
  - ❑ Stat: 0.5% at peak
  - ❑ Exp: 0.5% at peak
  - ❑ Lumi: 1.9%
- ➔ Plan simultaneous constraint on  $\sin^2\theta_W$  & PDF

Good agreement with Powheg+Py8 with CT10,  $m(l\bar{l})$  dependent NNLO QCD + NLO EWK k-factor (FEWZ) and  $pT(l\bar{l})$  and  $y(l\bar{l})$  dependent angular coefficient corrections at NNLO (DYNNLO)

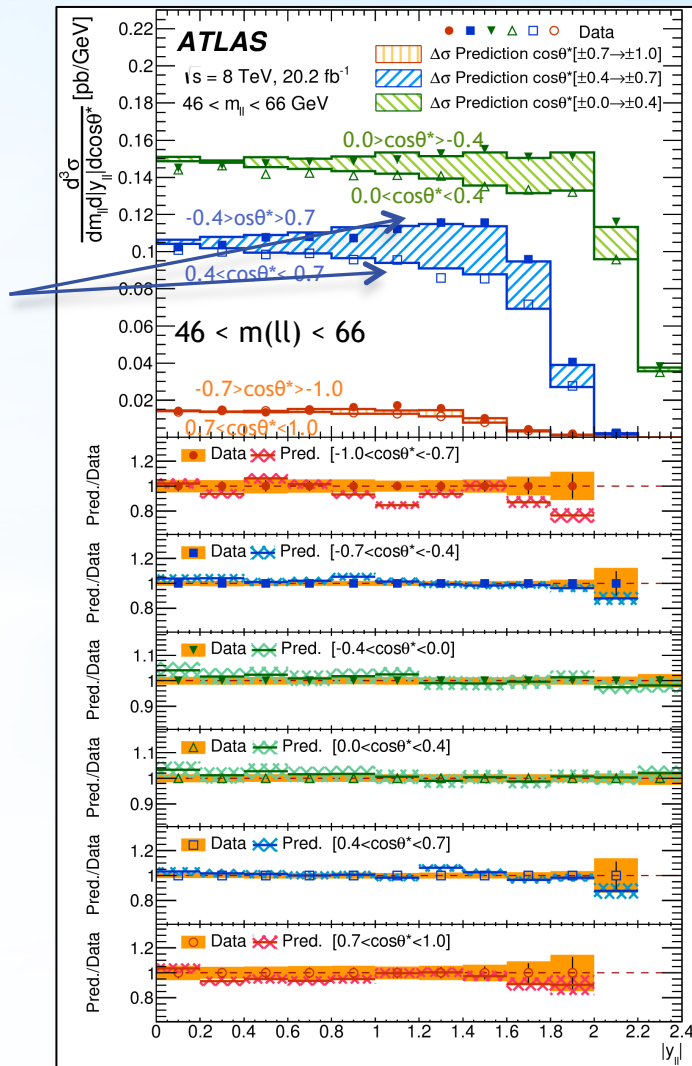
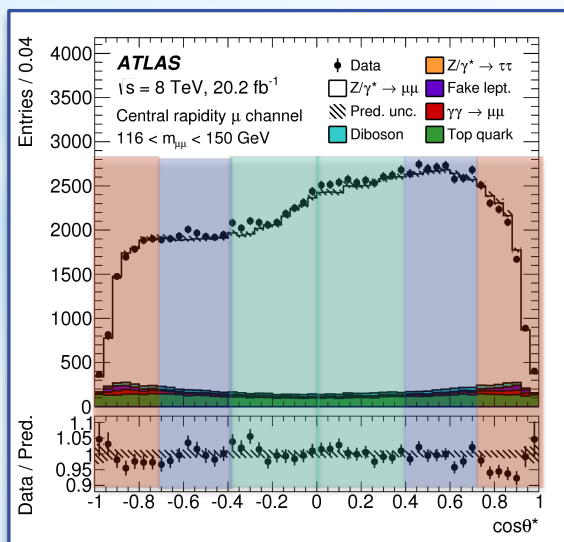


# Unfolded 3D DY cross sect.

Central+Central

FBA large  
for small  $m(l\bar{l})$

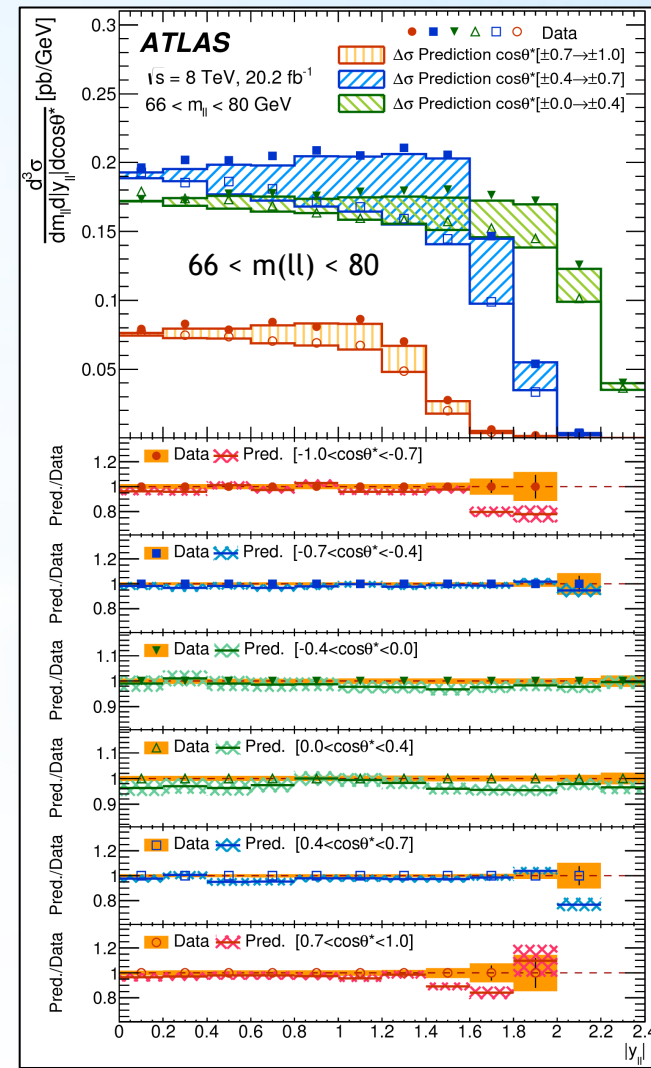
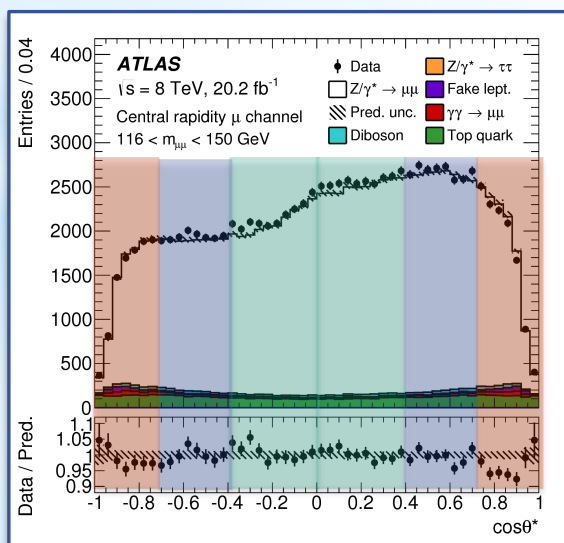
Forward-backward  
asymmetry



# Unfolded 3D DY cross sect.

Central+Central

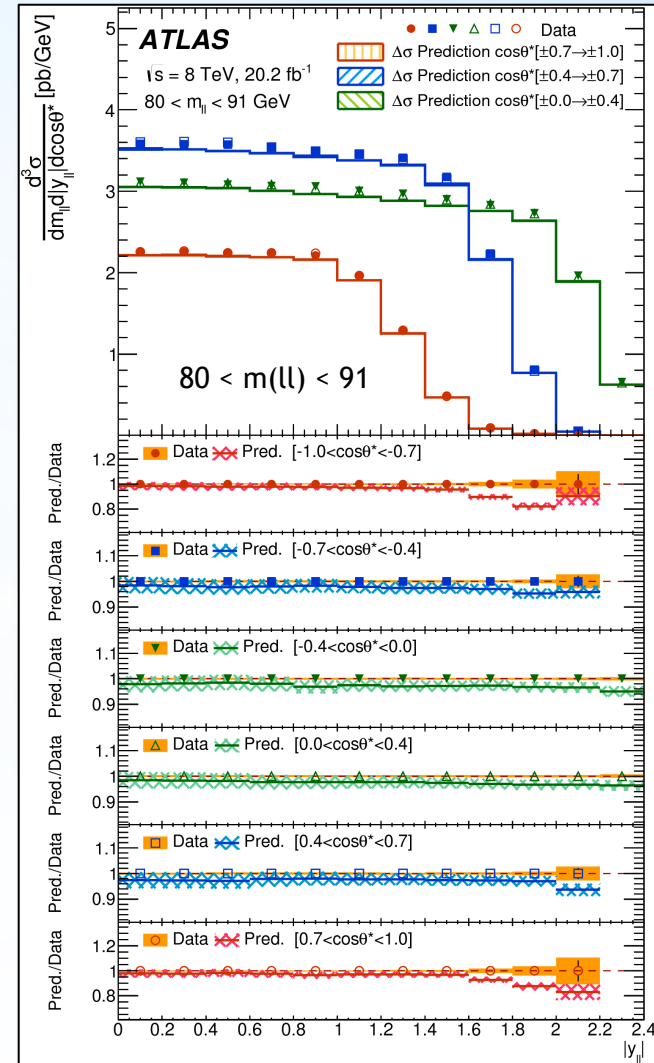
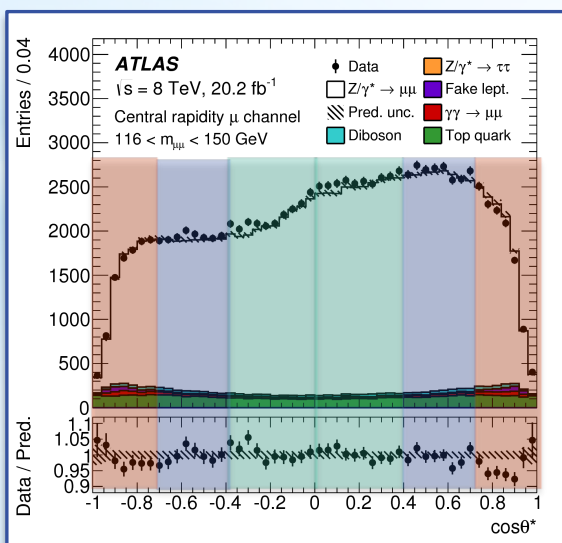
FBA large  
for small  $m(l\bar{l})$



# Unfolded 3D DY cross sect.

Central+Central

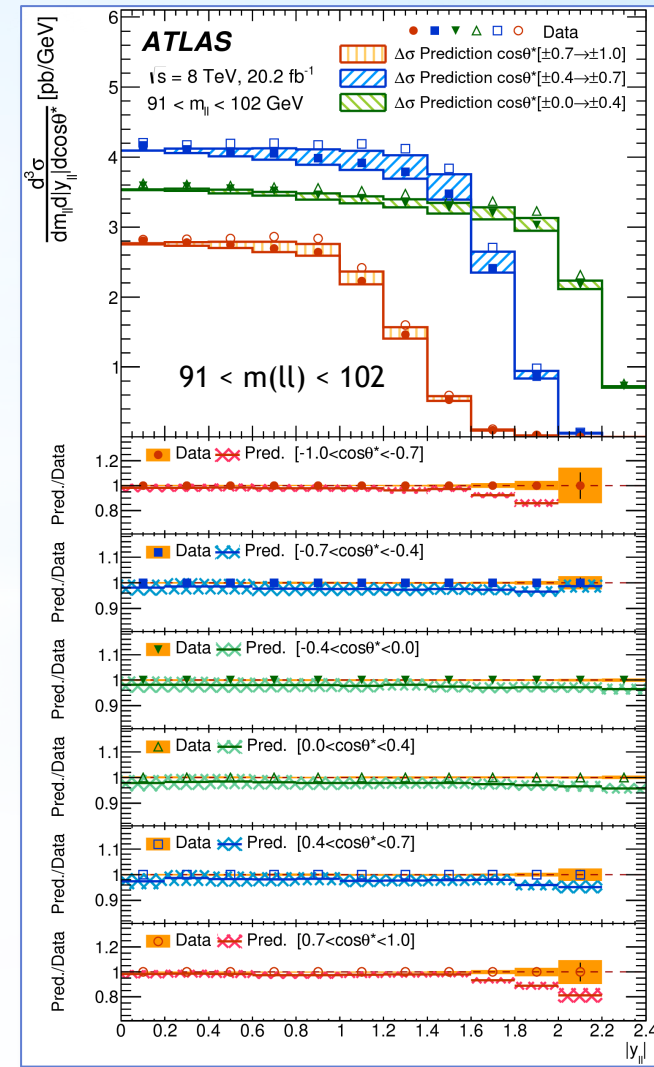
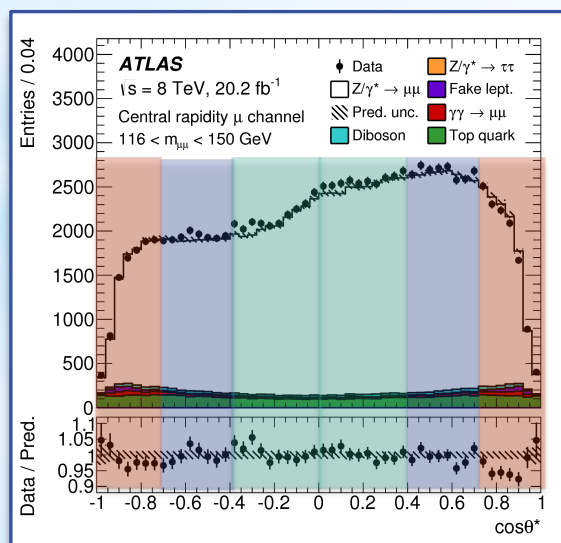
FBA vanishes  
at peak  
-> sign flip



# Unfolded 3D DY cross sect.

Central+Central

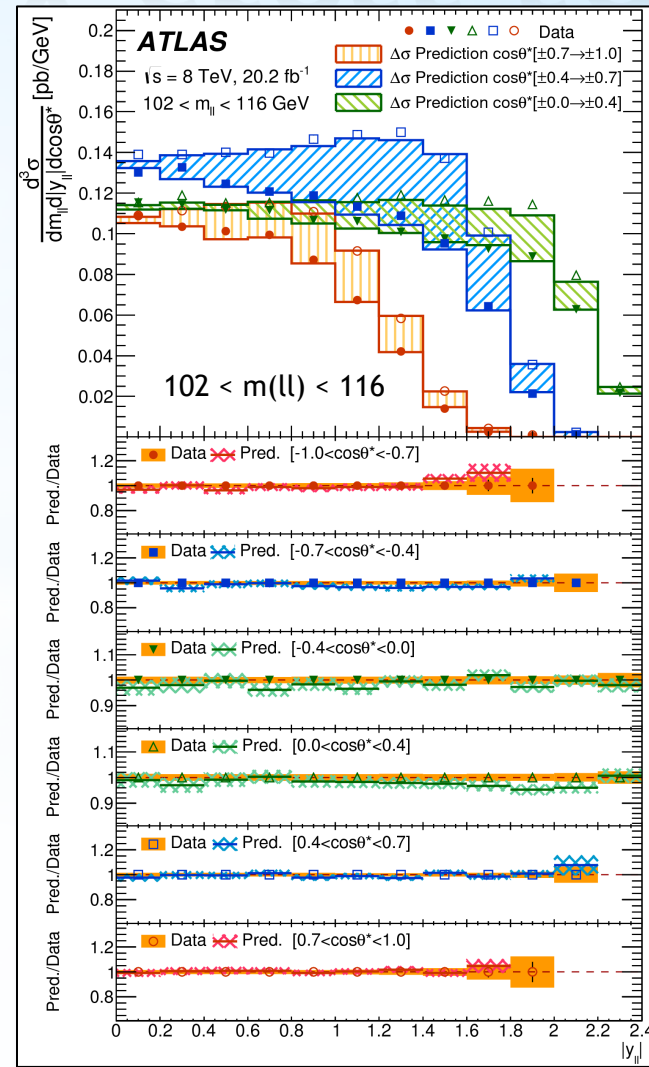
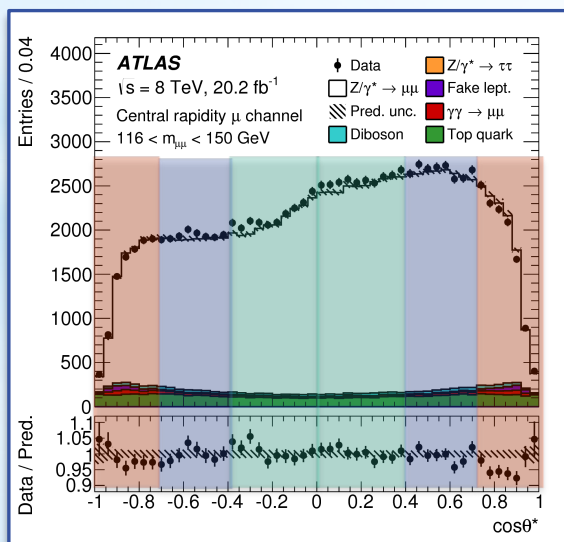
FBA vanishes  
at peak  
-> sign flip



# Unfolded 3D DY cross sect.

Central+Central

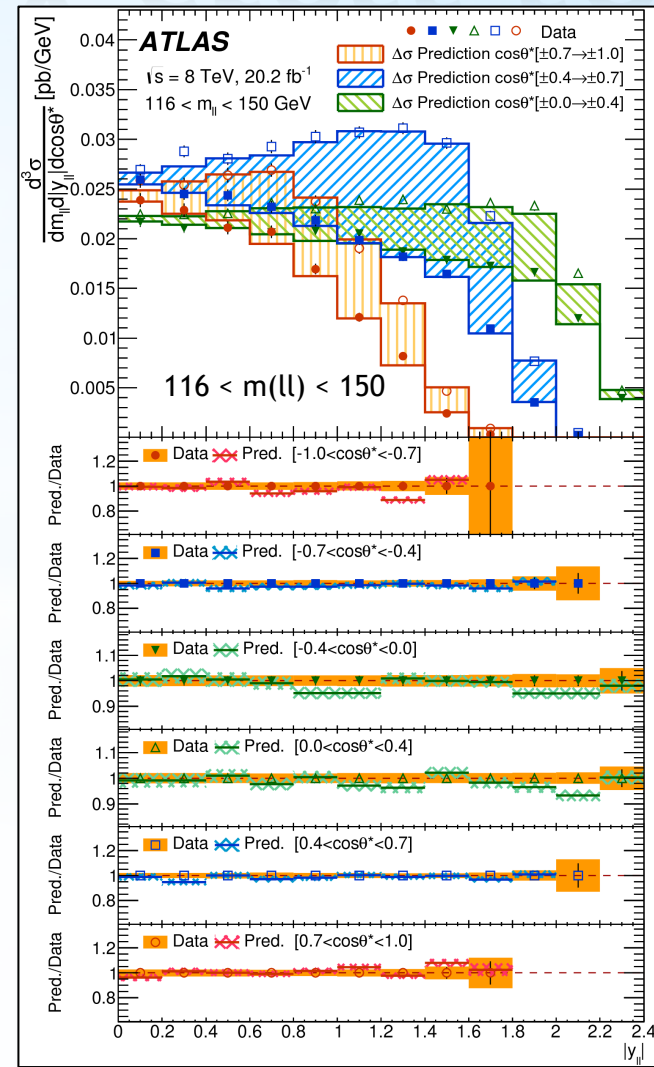
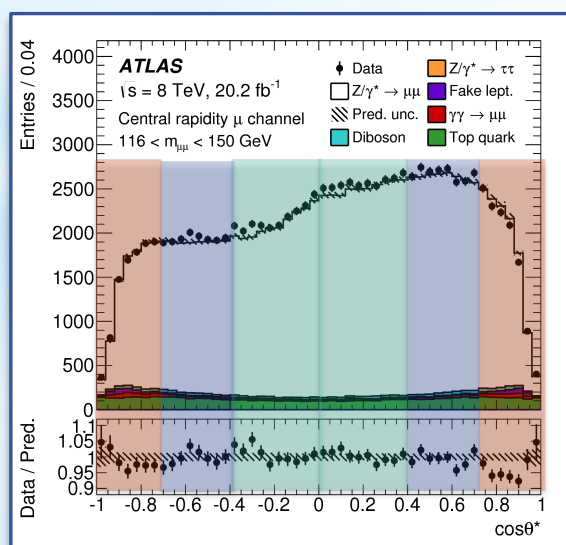
FBA large  
for large  $m(l\bar{l})$



# Unfolded 3D DY cross sect.

Central+Central

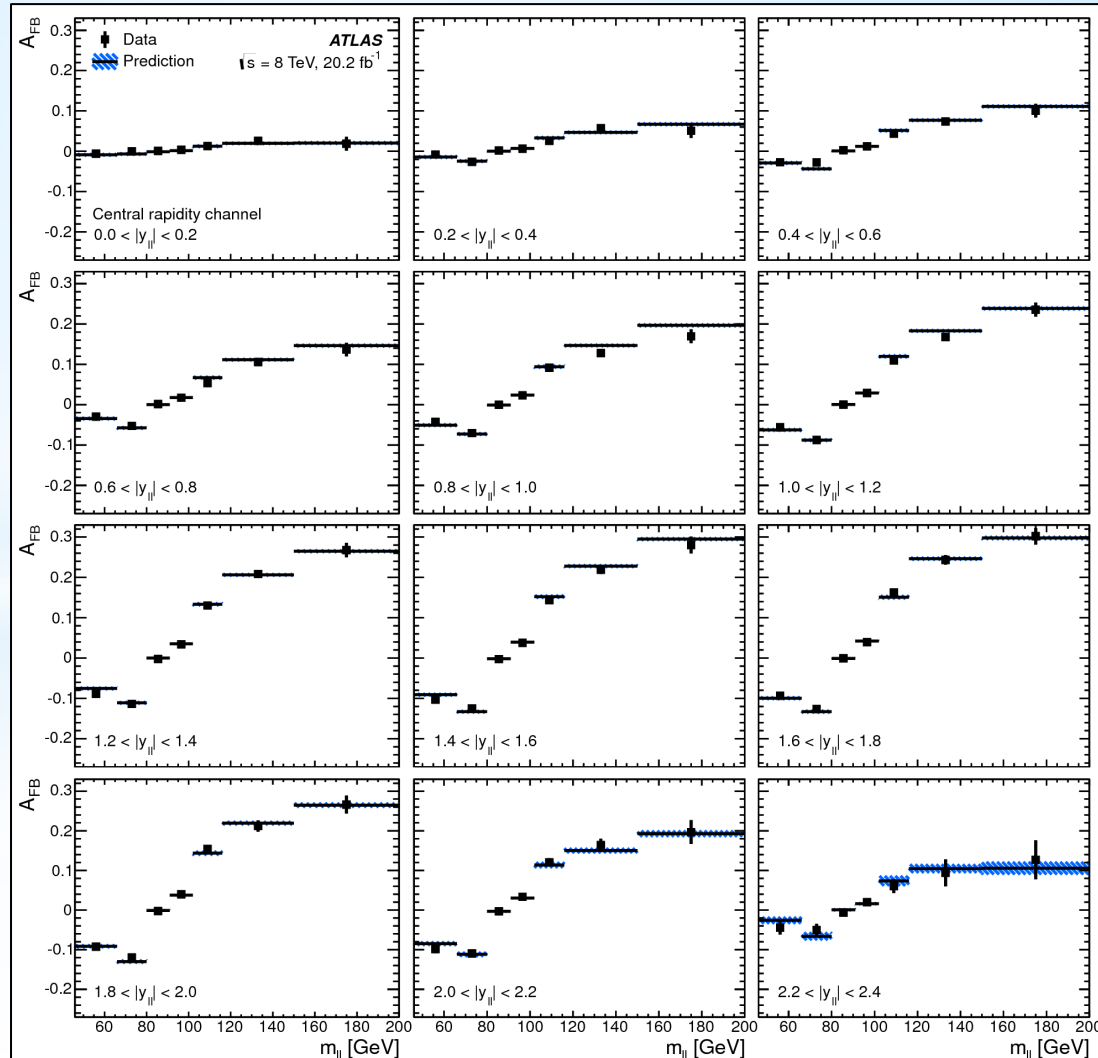
FBA large  
for large  $m(l\bar{l})$



# Unfolded 3D DY cross sect.

Central+Central

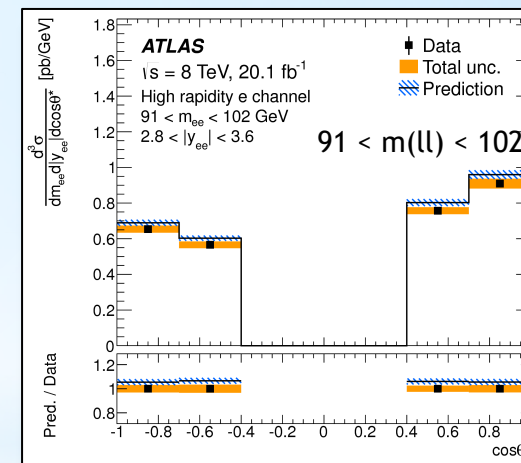
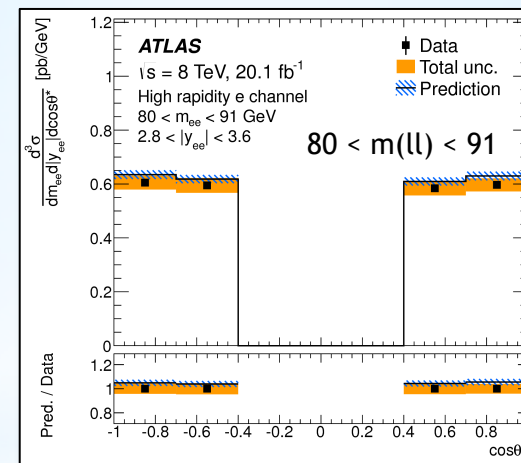
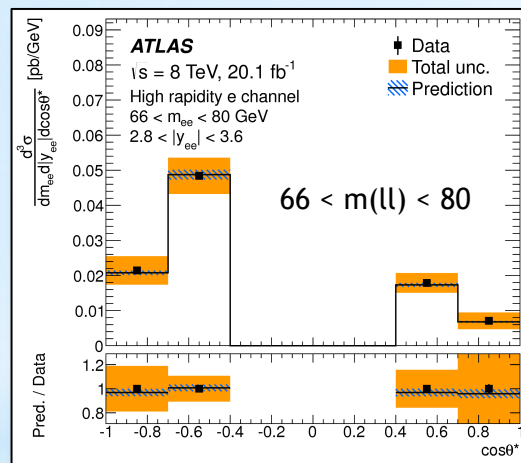
$$A_{FB} = \frac{\sigma_F - \sigma_B}{\sigma_F + \sigma_B}$$



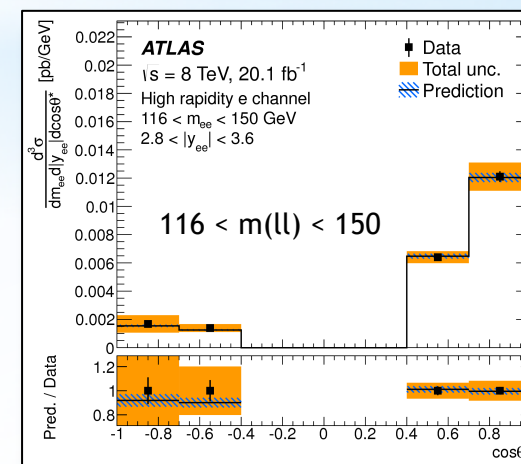
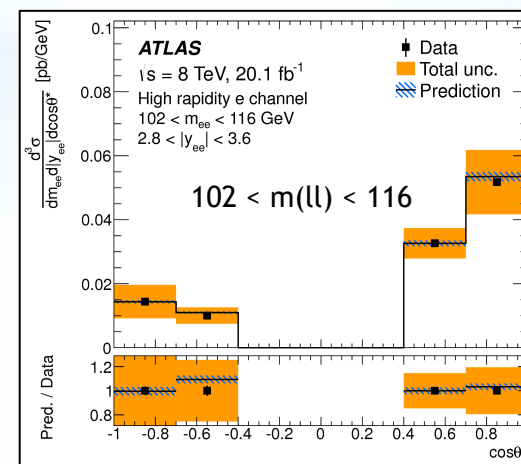
# Unfolded 3D DY cross sect.

# Central+Forward

Example:  $2.8 < y(\text{ll}) < 3.6$



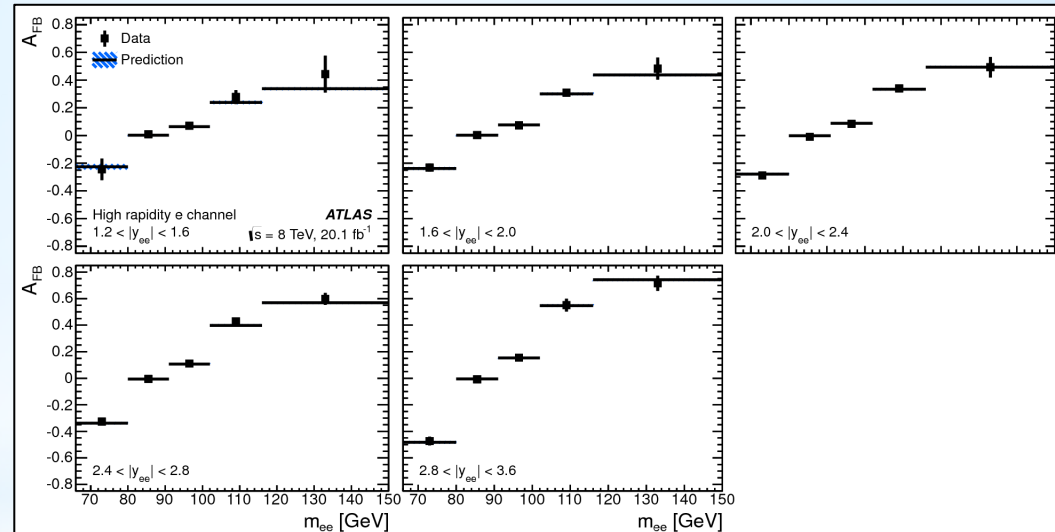
In electron channel up  
to  $y(ee) = 3.6$ :  
Most sensitive to  $\theta_w$   
(small dilution)



# Unfolded 3D DY cross sect.

Central+Forward

$$A_{FB} = \frac{\sigma_F - \sigma_B}{\sigma_F + \sigma_B}$$

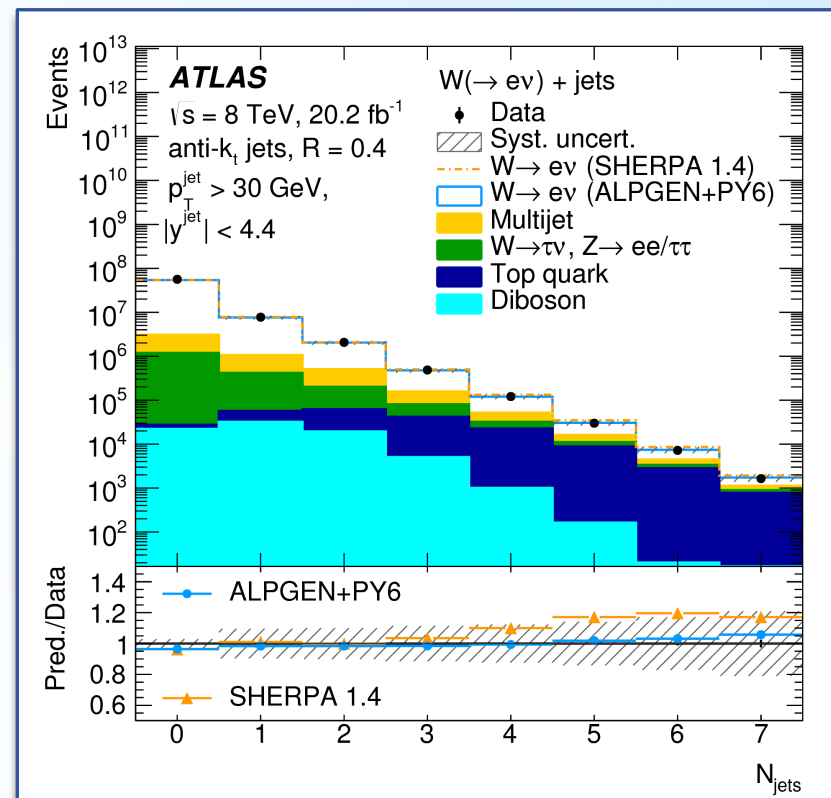


Measurements available in hepdata:  
<https://www.hepdata.net/record/77492>

# $W^+/W^- + \text{jets}$ cross sections

$$R_{\pm} = \frac{d\sigma(W^+)/dy_W}{d\sigma(W^-)/dy_W} = \frac{u(x_1)\bar{d}(x_2) + c(x_1)\bar{s}(x_2) + 1 \leftrightarrow 2}{d(x_1)\bar{u}(x_2) + s(x_1)\bar{c}(x_2) + 1 \leftrightarrow 2}$$

- ATLAS, 8TeV data (2012)
- W:  $p_T(e)$ ,  $\text{MET} > 25\text{GeV}$ ,  $mT > 40\text{GeV}$
- Jets:  $p_T > 30\text{GeV}$ ,  $|y| < 4.4$
- **Top bkg small due to b-veto**
- **Jet bkg 3-15% for  $W+0/1/2$  jets**
- Precision: 5-16% for  $W+0/1/2$  jets
  - JES, JER
  - Unfolding
- Precision, ratio: 0.7-4% for 0/1/2 jets
  - Jet background
  - MET
  - JER
- ➔ Publish unfolded cross section
- ➔ Ratios  $W^+/W^-$
- ➔ Sensitivity to PDF, in particular u/d



# $W^{\pm}/W^- + \text{jets}$ cross sections

$$R_{\pm} = \frac{d\sigma(W^+)/dy_W}{d\sigma(W^-)/dy_W} = \frac{u(x_1)\bar{d}(x_2) + c(x_1)\bar{s}(x_2) + 1 \leftrightarrow 2}{d(x_1)\bar{u}(x_2) + s(x_1)\bar{c}(x_2) + 1 \leftrightarrow 2}$$

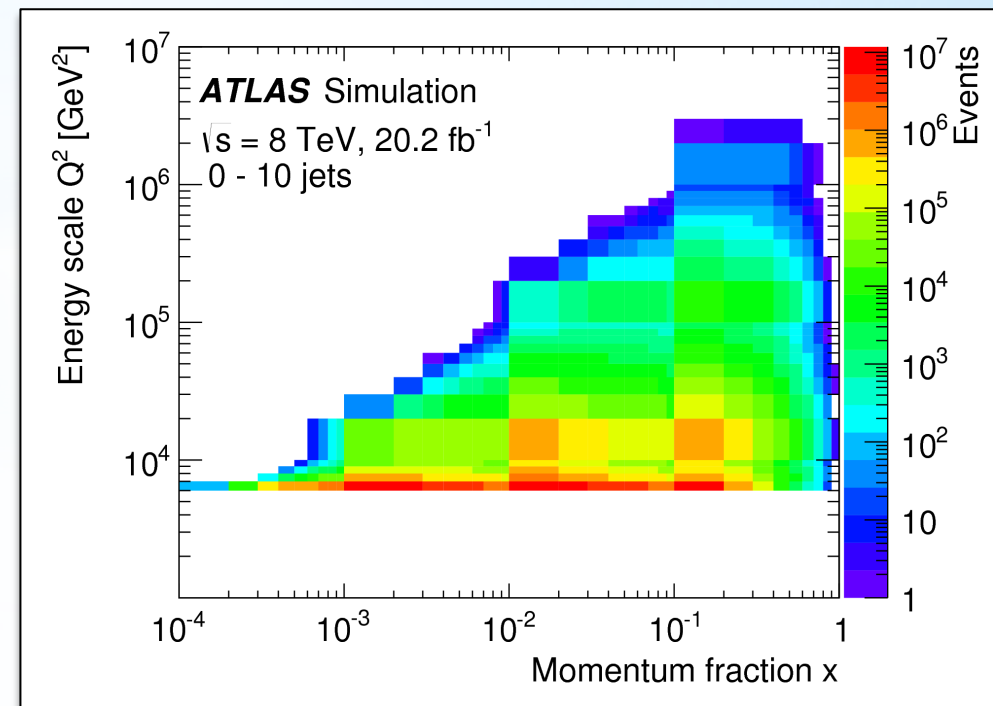
- ATLAS, 8TeV data (2012)
- W: pT(e), MET>25GeV, mT> 40GeV
- Jets: pT> 30GeV, |y|<4.4
- Top bkg small due to b-veto
- Jet bkg 3-15% for W+0/1/2 jets
- Precision: 5-16% for W+0/1/2 jets
  - JES, JER
  - Unfolding
- Precision, ratio: 0.7-4% for 0/1/2 jets
  - Jet background
  - MET
  - JER
- Publish unfolded cross section,
- Compare with selected predictions
- Ratios  $W^+/W^-$
- Sensitivity to PDF, in particular u/d

Program	Order in $\alpha_S$	$N_{\text{partons}}^{\max}$ at highest order	PDF set
$N_{\text{jetti}}$	NNLO	1	CT14
<b>BLACKHAT+SHERPA</b>	NLO	1, 2 or 3	CT10
<b>MCFM 6.8</b>	NLO	1	CT10 + 3 more
<b>POWHEG+PYTHIA 8</b>	NLO	1	CT14
<b>SHERPA 2.2.1</b>	NLO	2	CT10
<b>SHERPA 2.2.1</b>	LO	2 (3)	NNPDF 3.0
<b>ALPGEN+PYTHIA 6</b>	LO	5	CTEQ6L1 (LO)
<b>ALPGEN+HERWIG</b>	LO	5	CTEQ6L1 (LO)
<b>SHERPA 1.4.1</b>	LO	4	CT10

# $W^+/W^- + \text{jets}$ cross sections

$$R_{\pm} = \frac{d\sigma(W^+)/dy_W}{d\sigma(W^-)/dy_W} = \frac{u(x_1)\bar{d}(x_2) + c(x_1)\bar{s}(x_2) + 1 \leftrightarrow 2}{d(x_1)\bar{u}(x_2) + s(x_1)\bar{c}(x_2) + 1 \leftrightarrow 2}$$

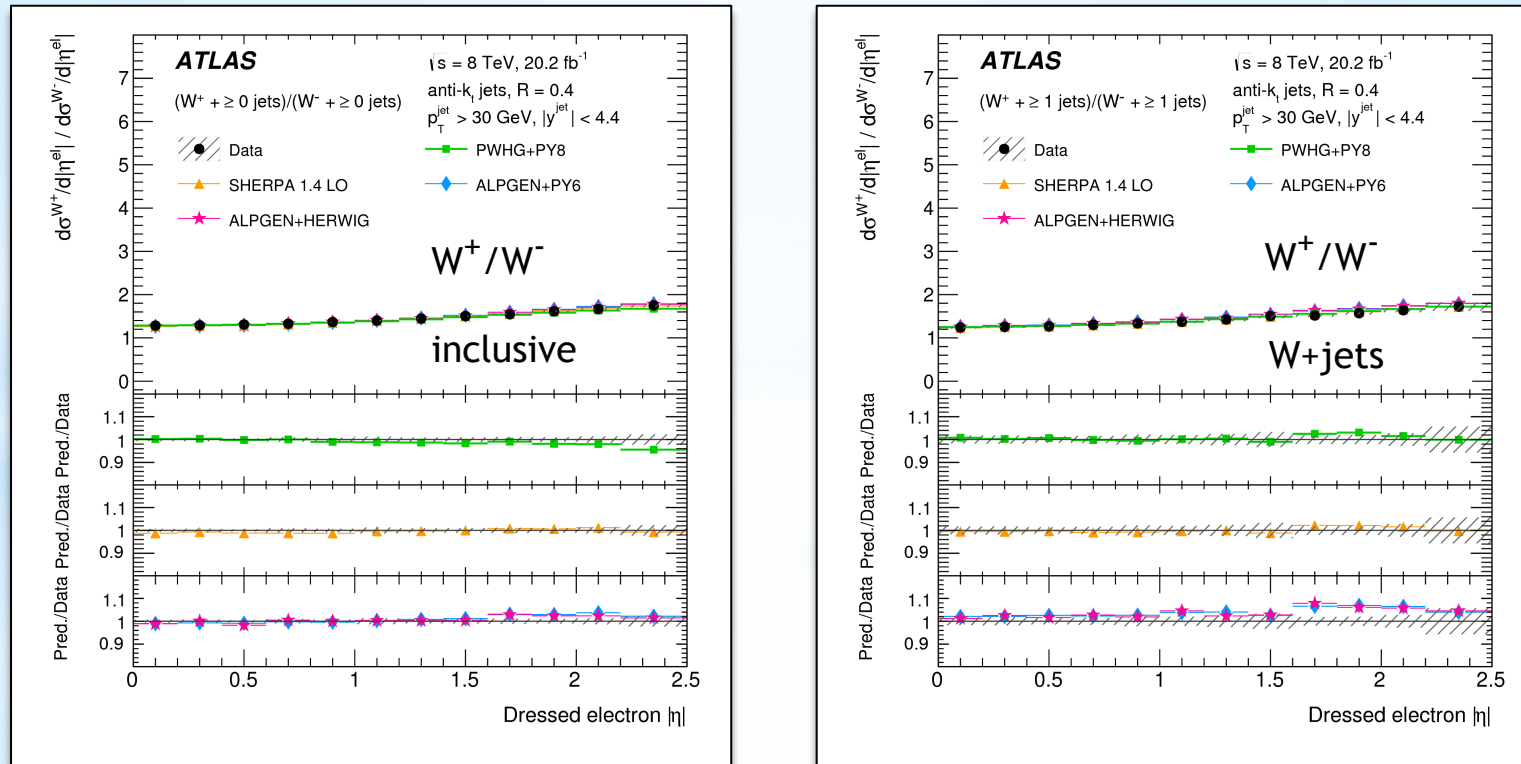
- ATLAS, 8TeV data (2012)
- W:  $pT(e)$ ,  $\text{MET} > 25\text{GeV}$ ,  $mT > 40\text{GeV}$
- Jets:  $pT > 30\text{GeV}$ ,  $|y| < 4.4$
- Top bkg small due to b-veto
- Jet bkg 3-15% for  $W+0/1/2$  jets
- Precision: 5-16% for  $W+0/1/2$  jets
  - JES, JER
  - Unfolding
- Precision, ratio: 0.7-4% for 0/1/2 jets
  - Jet background
  - MET
  - JER
- Publish unfolded cross section,
- Compare with selected predictions
- Ratios  $W^+/W^-$
- Sensitivity to PDF, in particular u/d



# $W^+/W^- + \text{jets}$ cross sections

*Analysis not optimized  
for inclusive  $W$  precision  
0.7% unc. on  $W^+/W^-$  ratio*

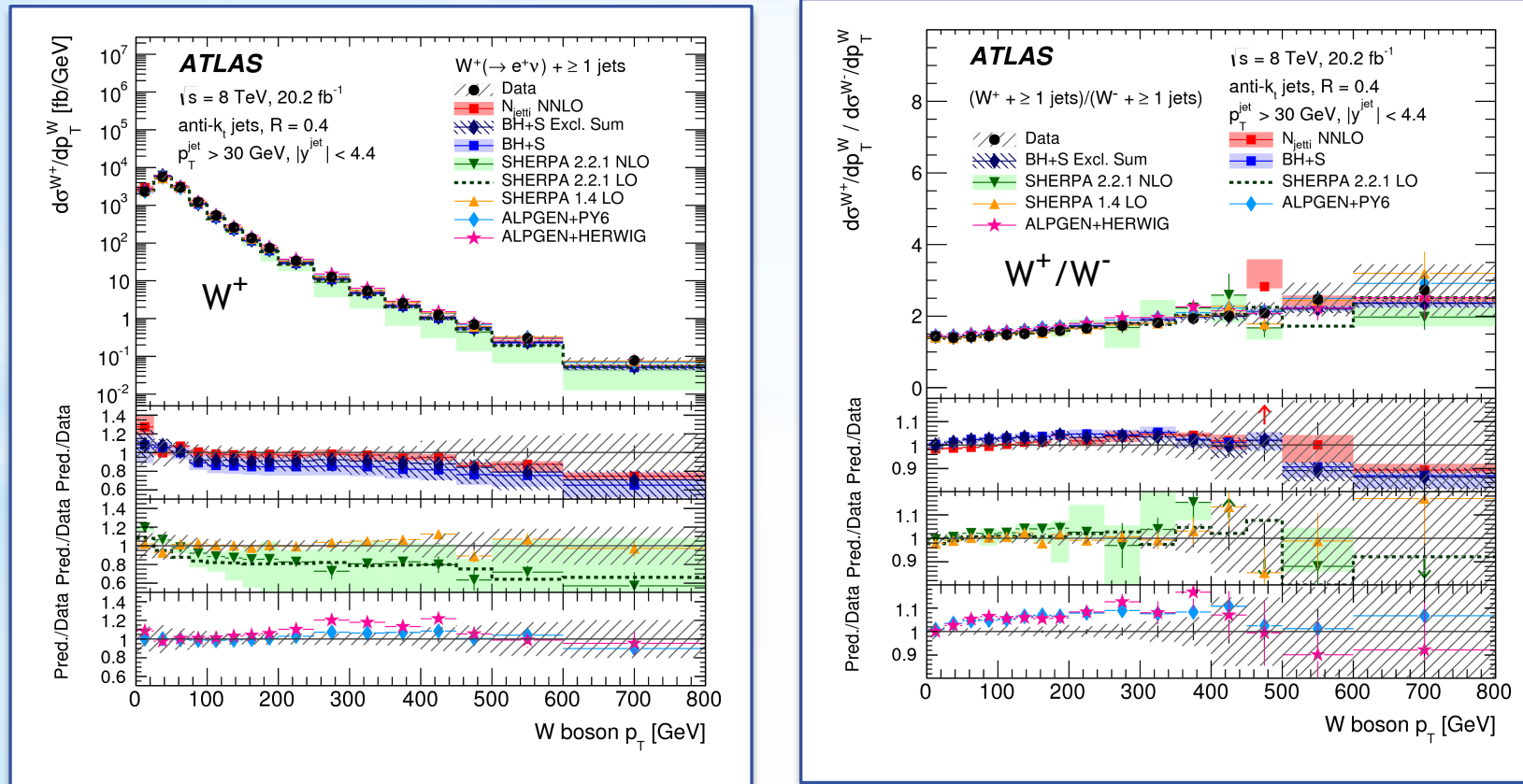
lepton  $|\eta|$



Good modeling by generators, asymmetry potentially sensitive to PDF

# $W^+/W^- + \text{jets}$ cross sections

$W + \text{jets}, p_T(W)$



NNLO/NLO fixed order and LO ME+PS consistent with data, some trends

# Summary

- Measurements of the Drell-Yan production of W and Z/gamma\* provide a benchmark of our understanding of perturbative QCD and probe the proton structure in a unique way.
- Most precise measurement at 7TeV now included in global fitters. Globally consistent, pulls strange sea in opposite direction to vs->lc data towards unsuppressed strange sea.
- New set of high precision measurements at 8 TeV:
  - Precise triple differential cross-section measurement as a function of Mll, dilepton rapidity and  $\cos\theta^*$  -> sensitivity to the PDFs and the Z forward-backward asymmetry, AFB
  - W+/W- ratios now as well in W+jets, as a function of several observables

# Appendix

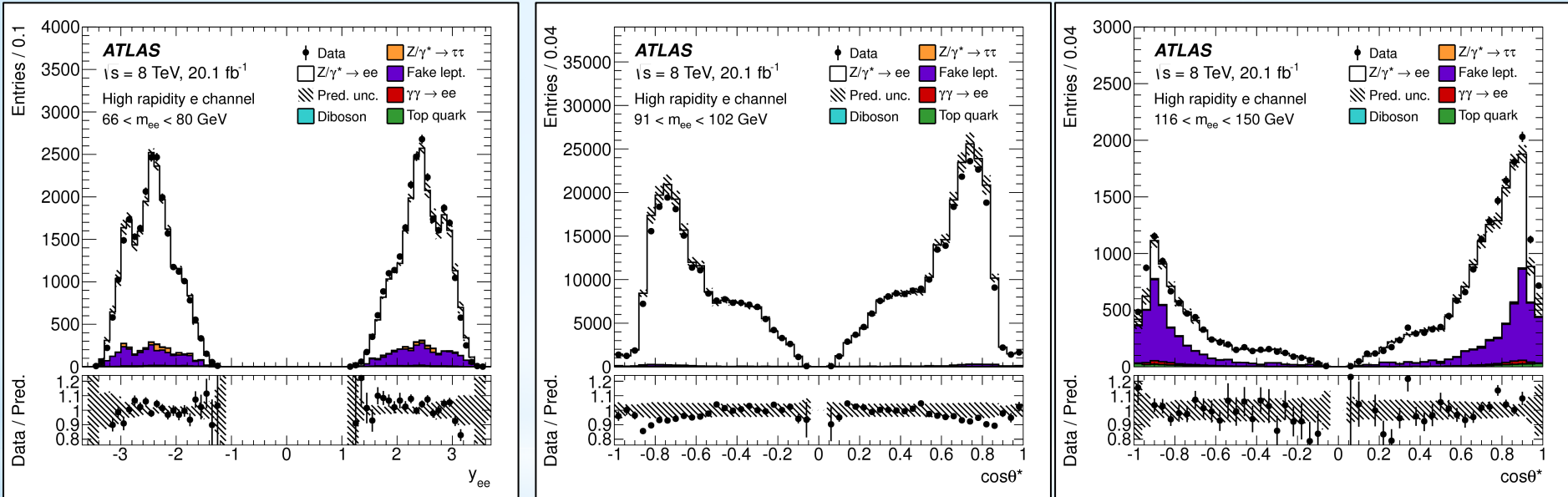
# Appendix

$$\frac{d^3\sigma}{dm_{\ell\ell}dy_{\ell\ell}d\cos\theta^*} = \frac{\pi\alpha^2}{3m_{\ell\ell}s} \sum_q P_q [f_q(x_1, Q^2)f_{\bar{q}}(x_2, Q^2) + (q \leftrightarrow \bar{q})]$$

$$\begin{aligned} P_q &= e_\ell^2 e_q^2 (1 + \cos^2 \theta^*) \\ &+ e_\ell e_q \frac{2m_{\ell\ell}^2(m_{\ell\ell}^2 - m_Z^2)}{\sin^2 \theta_W \cos^2 \theta_W [(m_{\ell\ell}^2 - m_Z^2)^2 + \Gamma_Z^2 m_Z^2]} [v_\ell v_q (1 + \cos^2 \theta^*) + 2a_\ell a_q \cos \theta^*] \\ &+ \frac{m_{\ell\ell}^4}{\sin^4 \theta_W \cos^4 \theta_W [(m_{\ell\ell}^2 - m_Z^2)^2 + \Gamma_Z^2 m_Z^2]} [(a_\ell^2 + v_\ell^2)(a_q^2 + v_q^2)(1 + \cos^2 \theta^*) + 8a_\ell v_\ell a_q v_q \cos \theta^*]. \end{aligned}$$

$$d^3\sigma \equiv \frac{d^3\sigma}{dm_{\ell\ell}dy_{\ell\ell}d\cos\theta^*}$$

# Appendix



# Appendix

Process	Generator	Parton shower & underlying event	Generator PDF	Model parameters (“Tune”)
$Z/\gamma^* \rightarrow \ell\ell$	Powheg v1(r1556)	Pythia 8.162	CT10	AU2 [62]
$Z/\gamma^* \rightarrow \tau\tau$	Powheg v1(r1556)	Pythia 8.162	CT10	AU2
$\gamma\gamma \rightarrow \ell\ell$	Pythia 8.170	Pythia 8.170	MRST2004qed	4C [63]
$t\bar{t}$	Powheg v1(r1556)	Pythia 6.427.2	CT10	AUET2 [64]
$Wt$	Powheg v1(r1556)	Pythia 6.427.2	CT10	AUET2
Diboson	Herwig 6.520	Herwig 6.520	CTEQ6L1	AUET2
$W \rightarrow \ell\nu$	Powheg v1(r1556)	Pythia 8.162	CT10	AU2

Bin	$m_{ee}$ [GeV]	$ y_{ee} $	$\cos \theta^*$	$\delta_{\text{unc}}^{\text{stat}}$ [%]	$\delta_{\text{unc}}^{\text{sig}}$ [%]	$\delta_{\text{unc}}^{\text{bkg}}$ [%]	$\delta_{\text{unc}}^{\text{mj}}$ [%]	$\delta_{\text{cor}}^{\text{bkg}}$ [%]	$\delta_{\text{cor}}^{\text{mj}}$ [%]	$\delta_{\text{cor}}^{\text{scl}}$ [%]	$\delta_{\text{cor}}^{\text{res}}$ [%]	$\delta_{\text{cor}}^{\text{rec}}$ [%]	$\delta_{\text{cor}}^{\text{id}}$ [%]	$\delta_{\text{cor}}^{\text{trig}}$ [%]	$\delta_{\text{cor}}^{\text{qmid}}$ [%]	$\delta_{\text{cor}}^{\text{kfac}}$ [%]	$\delta_{\text{cor}}^{\text{zpt}}$ [%]	$\delta_{\text{cor}}^{\text{pdf}}$ [%]	$\delta^{\text{tot}}$ [%]
1	46, 66	0.0, 0.2	-1.0, -0.7	6.7	2.4	3.4	3.1	1.9	5.2	0.5	0.7	0.5	2.5	0.7	0.2	0.0	0.9	0.2	10.6
2	46, 66	0.0, 0.2	-0.7, -0.4	2.3	0.8	1.2	0.9	1.1	2.0	0.2	0.2	0.5	2.7	0.9	0.0	0.0	0.0	0.1	4.7
3	46, 66	0.0, 0.2	-0.4, 0.0	1.4	0.5	0.9	0.4	0.9	0.9	0.3	0.1	0.3	1.9	0.3	0.0	0.0	0.0	0.0	2.9
4	46, 66	0.0, 0.2	0.0, +0.4	1.4	0.5	0.8	0.5	0.9	0.9	0.3	0.1	0.3	1.9	0.3	0.0	0.0	0.0	0.1	3.0
5	46, 66	0.0, 0.2	+0.4, +0.7	2.2	0.8	0.9	0.9	1.1	2.0	0.2	0.1	0.5	2.6	0.8	0.0	0.0	0.0	0.1	4.5
6	46, 66	0.0, 0.2	+0.7, +1.0	6.7	2.3	4.8	3.1	1.8	4.9	0.9	0.5	0.5	2.6	0.7	0.1	0.0	0.9	0.2	10.9
79	66, 80	0.2, 0.4	-1.0, -0.7	2.7	1.3	0.5	0.7	0.5	1.6	1.5	1.1	0.6	3.7	1.2	0.1	0.0	0.3	0.2	5.6
80	66, 80	0.2, 0.4	-0.7, -0.4	1.3	0.6	0.4	0.3	0.3	0.3	0.4	0.4	0.3	1.7	0.4	0.1	0.0	0.0	0.0	2.5
81	66, 80	0.2, 0.4	-0.4, 0.0	1.3	0.4	0.4	0.3	0.3	0.1	0.3	0.1	0.1	0.7	0.2	0.0	0.0	0.0	0.0	1.6
82	66, 80	0.2, 0.4	0.0, +0.4	1.2	0.5	0.3	0.4	0.3	0.1	0.3	0.1	0.1	0.7	0.2	0.1	0.0	0.0	0.0	1.7
83	66, 80	0.2, 0.4	+0.4, +0.7	1.4	0.6	0.3	0.3	0.3	0.6	0.2	0.3	1.7	0.4	0.1	0.0	0.1	0.0	0.0	2.6
84	66, 80	0.2, 0.4	+0.7, +1.0	2.7	1.4	0.4	0.7	0.4	1.6	2.8	1.0	0.6	3.8	1.2	0.2	0.0	0.3	0.1	6.1
157	80, 91	0.4, 0.6	-1.0, -0.7	0.6	0.3	0.0	0.1	0.0	0.1	1.4	0.3	0.3	3.2	0.4	0.1	0.0	0.0	0.1	3.6
158	80, 91	0.4, 0.6	-0.7, -0.4	0.4	0.2	0.0	0.0	0.0	0.0	1.0	0.1	0.1	0.5	0.2	0.1	0.0	0.1	0.0	1.2
159	80, 91	0.4, 0.6	-0.4, 0.0	0.4	0.1	0.0	0.0	0.0	0.0	1.0	0.1	0.0	0.3	0.1	0.1	0.0	0.0	0.0	1.1
160	80, 91	0.4, 0.6	0.0, +0.4	0.4	0.1	0.0	0.0	0.0	0.0	1.0	0.0	0.0	0.3	0.1	0.1	0.0	0.0	0.0	1.2
161	80, 91	0.4, 0.6	+0.4, +0.7	0.4	0.2	0.0	0.0	0.0	0.0	1.0	0.1	0.1	0.5	0.2	0.1	0.0	0.1	0.0	1.2
162	80, 91	0.4, 0.6	+0.7, +1.0	0.6	0.3	0.0	0.0	0.0	0.1	1.6	0.2	0.3	3.2	0.4	0.1	0.0	0.0	0.1	3.7
235	91, 102	0.6, 0.8	-1.0, -0.7	0.5	0.2	0.0	0.1	0.0	0.0	2.1	0.2	0.3	2.6	0.5	0.0	0.0	0.2	0.0	3.5
236	91, 102	0.6, 0.8	-0.7, -0.4	0.4	0.2	0.0	0.0	0.0	0.0	1.3	0.0	0.1	0.5	0.2	0.0	0.0	0.1	0.0	1.5
237	91, 102	0.6, 0.8	-0.4, 0.0	0.4	0.1	0.0	0.0	0.0	0.0	1.0	0.1	0.0	0.2	0.1	0.0	0.0	0.0	0.0	1.1
238	91, 102	0.6, 0.8	0.0, +0.4	0.3	0.1	0.0	0.0	0.0	0.0	1.0	0.0	0.0	0.2	0.1	0.0	0.0	0.0	0.0	1.1
239	91, 102	0.6, 0.8	+0.4, +0.7	0.4	0.2	0.0	0.0	0.0	0.0	1.2	0.0	0.1	0.5	0.2	0.0	0.0	0.1	0.0	1.4
240	91, 102	0.6, 0.8	+0.7, +1.0	0.5	0.2	0.0	0.1	0.0	0.1	2.1	0.1	0.3	2.6	0.5	0.0	0.0	0.2	0.0	3.4
313	102, 116	0.8, 1.0	-1.0, -0.7	2.8	1.2	0.6	0.8	0.5	0.7	2.1	0.9	0.2	1.4	0.3	0.1	0.0	0.1	0.0	4.3
314	102, 116	0.8, 1.0	-0.7, -0.4	2.6	1.2	0.2	0.5	0.2	0.9	2.3	1.0	0.0	0.4	0.2	0.0	0.0	0.1	0.1	4.0
315	102, 116	0.8, 1.0	-0.4, 0.0	2.0	0.8	1.6	0.3	0.2	0.2	1.0	0.3	0.1	0.3	0.1	0.1	0.0	0.0	0.0	2.9
316	102, 116	0.8, 1.0	0.0, +0.4	1.8	0.7	0.1	0.2	0.2	0.1	0.9	0.5	0.1	0.3	0.1	0.0	0.0	0.1	0.1	2.2
317	102, 116	0.8, 1.0	+0.4, +0.7	2.3	1.0	0.5	0.4	0.2	0.7	1.7	1.3	0.0	0.4	0.2	0.1	0.0	0.0	0.1	3.5
318	102, 116	0.8, 1.0	+0.7, +1.0	2.3	1.0	0.2	0.6	0.3	0.6	2.1	0.6	0.2	1.4	0.3	0.0	0.0	0.0	0.1	3.8
391	116, 150	1.0, 1.2	-1.0, -0.7	4.8	1.0	2.8	1.8	1.3	5.1	0.2	0.4	0.1	0.4	0.2	0.1	0.0	0.0	0.1	8.0
392	116, 150	1.0, 1.2	-0.7, -0.4	3.5	0.9	0.4	0.7	0.7	0.6	0.6	0.1	0.1	0.3	0.2	0.1	0.0	0.2	0.1	3.9
393	116, 150	1.0, 1.2	-0.4, 0.0	3.1	0.8	1.3	0.4	0.5	0.8	0.6	0.1	0.1	0.4	0.2	0.1	0.0	0.0	0.2	3.7
394	116, 150	1.0, 1.2	0.0, +0.4	3.0	0.8	0.6	0.5	0.4	0.9	0.6	0.2	0.1	0.4	0.2	0.1	0.0	0.1	0.0	3.5
395	116, 150	1.0, 1.2	+0.4, +0.7	2.8	0.7	0.5	0.5	0.4	0.6	0.4	0.1	0.3	0.2	0.1	0.0	0.1	0.1	0.1	3.2
396	116, 150	1.0, 1.2	+0.7, +1.0	3.7	0.8	2.2	1.1	0.8	3.4	0.4	0.2	0.1	0.4	0.2	0.1	0.0	0.0	0.1	5.7
469	150, 200	1.2, 1.4	-1.0, -0.7	11.9	1.4	2.0	3.6	2.2	1.5	0.4	0.3	0.1	0.5	0.3	0.1	0.0	0.0	0.2	12.9
470	150, 200	1.2, 1.4	-0.7, -0.4	6.6	0.8	1.0	5.9	1.6	0.9	0.9	0.2	0.1	0.5	0.3	0.1	0.0	0.0	0.1	9.2
471	150, 200	1.2, 1.4	-0.4, 0.0	6.6	1.0	3.1	1.9	1.0	0.4	1.0	0.1	0.2	0.6	0.3	0.2	0.0	0.0	0.1	7.8
472	150, 200	1.2, 1.4	0.0, +0.4	5.3	0.9	0.8	0.9	0.6	0.2	0.6	0.2	0.2	0.6	0.3	0.2	0.0	0.1	0.0	5.6
473	150, 200	1.2, 1.4	+0.4, +0.7	4.4	0.6	0.5	1.9	0.7	0.4	0.9	0.2	0.1	0.5	0.3	0.1	0.0	0.0	0.0	5.0
474	150, 200	1.2, 1.4	+0.7, +1.0	7.6	0.9	1.1	2.3	1.1	0.7	0.3	0.2	0.1	0.5	0.3	0.2	0.0	0.0	0.1	8.3

Bin	$m_{ee}$ [GeV]	$ y_{ee} $	$\cos \theta^*$	$\delta_{\text{unc}}^{\text{stat}}$ [%]	$\delta_{\text{unc}}^{\text{sig}}$ [%]	$\delta_{\text{unc}}^{\text{bkg}}$ [%]	$\delta_{\text{unc}}^{\text{mj}}$ [%]	$\delta_{\text{cor}}^{\text{bkg}}$ [%]	$\delta_{\text{cor}}^{\text{mj}}$ [%]	$\delta_{\text{cor}}^{\text{scl}}$ [%]	$\delta_{\text{cor}}^{\text{res}}$ [%]	$\delta_{\text{cor}}^{\text{fsc}}$ [%]	$\delta_{\text{cor}}^{\text{fres}}$ [%]	$\delta_{\text{cor}}^{\text{rec}}$ [%]	$\delta_{\text{cor}}^{\text{id}}$ [%]	$\delta_{\text{cor}}^{\text{trig}}$ [%]	$\delta_{\text{cor}}^{\text{iso}}$ [%]	$\delta_{\text{cor}}^{\text{fid}}$ [%]	$\delta_{\text{cor}}^{\text{qmid}}$ [%]	$\delta_{\text{cor}}^{\text{kfac}}$ [%]	$\delta_{\text{cor}}^{\text{zpt}}$ [%]	$\delta_{\text{cor}}^{\text{pdf}}$ [%]	$\delta_{\text{tot}}$ [%]
1	66, 80	1.2, 1.6	-1.0, -0.7	6.4	3.0	6.0	4.5	0.9	11.5	0.4	0.6	3.1	2.1	0.2	0.8	0.3	0.0	0.7	0.0	0.0	0.8	0.6	16.0
2	66, 80	1.2, 1.6	-0.7, -0.4	16.4	8.7	8.0	9.9	0.5	11.4	0.5	1.2	5.8	2.5	0.1	0.2	0.1	0.0	0.8	0.0	0.0	0.8	0.3	26.0
3	66, 80	1.2, 1.6	-0.4, 0.0	-	-	-	-	-	-	-	-	-	-	-	-	-	-	-	-	-	-	-	
4	66, 80	1.2, 1.6	0.0, +0.4	-	-	-	-	-	-	-	-	-	-	-	-	-	-	-	-	-	-	-	
5	66, 80	1.2, 1.6	+0.4, +0.7	15.7	8.0	6.7	7.9	0.5	10.7	0.9	0.8	3.8	5.5	0.1	0.1	0.1	0.0	0.8	0.0	0.0	1.6	1.4	24.1
6	66, 80	1.2, 1.6	+0.7, +1.0	7.9	3.3	8.8	5.8	1.6	15.3	0.7	0.7	2.3	2.9	0.2	0.8	0.3	0.0	0.7	0.0	0.0	0.9	0.3	20.9
19	66, 80	2.4, 2.8	-1.0, -0.7	3.4	2.2	1.4	2.8	0.3	3.4	2.5	0.7	4.3	5.2	0.2	1.6	0.4	0.1	1.4	0.0	0.0	2.4	0.2	10.1
20	66, 80	2.4, 2.8	-0.7, -0.4	2.2	1.3	0.8	1.6	0.3	1.1	1.2	0.6	3.1	3.9	0.1	0.8	0.2	0.0	1.3	0.0	0.0	0.5	0.1	6.4
21	66, 80	2.4, 2.8	-0.4, 0.0	2.3	1.0	0.8	1.4	0.2	1.5	0.4	0.2	0.9	0.3	0.1	0.5	0.2	0.0	0.8	0.0	0.0	0.1	0.0	3.6
22	66, 80	2.4, 2.8	0.0, +0.4	2.8	1.2	1.5	1.9	0.4	2.0	0.4	0.5	1.3	0.3	0.1	0.5	0.2	0.0	0.7	0.0	0.0	0.3	0.1	4.7
23	66, 80	2.4, 2.8	+0.4, +0.7	2.7	1.6	1.3	2.3	0.4	1.7	1.6	0.2	4.0	6.0	0.1	0.8	0.2	0.0	1.4	0.1	0.0	1.1	0.2	8.8
24	66, 80	2.4, 2.8	+0.7, +1.0	4.2	2.7	3.4	3.7	0.7	5.5	2.8	0.9	4.9	6.5	0.2	1.6	0.4	0.1	1.4	0.0	0.0	3.6	0.3	13.2
73	91, 102	2.0, 2.4	-1.0, -0.7	0.9	0.6	0.2	0.3	0.0	0.8	0.8	0.1	1.9	0.1	0.2	0.8	0.2	0.0	1.2	0.0	0.0	0.8	0.1	2.9
74	91, 102	2.0, 2.4	-0.7, -0.4	0.5	0.3	0.0	0.2	0.0	0.7	0.9	0.1	1.5	0.2	0.0	0.4	0.1	0.0	0.8	0.0	0.0	0.1	0.1	2.1
75	91, 102	2.0, 2.4	-0.4, 0.0	0.7	0.3	0.1	0.4	0.0	0.6	0.6	0.1	1.7	0.1	0.0	0.2	0.1	0.0	0.7	0.0	0.0	0.1	0.0	2.2
76	91, 102	2.0, 2.4	0.0, +0.4	0.6	0.3	0.1	0.4	0.0	0.5	0.5	0.1	1.5	0.1	0.0	0.2	0.1	0.0	0.7	0.0	0.0	0.1	0.1	2.0
77	91, 102	2.0, 2.4	+0.4, +0.7	0.5	0.3	0.1	0.1	0.0	0.5	0.9	0.2	1.3	0.3	0.0	0.4	0.1	0.0	0.8	0.0	0.0	0.2	0.1	2.0
78	91, 102	2.0, 2.4	+0.7, +1.0	0.9	0.5	0.2	0.3	0.0	0.3	0.7	0.2	1.6	0.2	0.2	0.7	0.2	0.0	1.2	0.0	0.0	0.8	0.0	2.6
97	102, 116	1.6, 2.0	-1.0, -0.7	3.8	1.8	2.0	2.9	0.7	4.2	0.6	0.3	2.4	2.2	0.1	0.3	0.1	0.0	0.8	0.0	0.0	1.5	0.1	7.9
98	102, 116	1.6, 2.0	-0.7, -0.4	4.4	2.1	2.0	3.4	0.3	3.6	1.2	0.6	2.1	1.2	0.0	0.2	0.0	0.0	0.7	0.0	0.0	1.5	0.2	8.0
99	102, 116	1.6, 2.0	-0.4, 0.0	-	-	-	-	-	-	-	-	-	-	-	-	-	-	-	-	-	-	-	
100	102, 116	1.6, 2.0	0.0, +0.4	-	-	-	-	-	-	-	-	-	-	-	-	-	-	-	-	-	-	-	
101	102, 116	1.6, 2.0	+0.4, +0.7	3.3	1.5	1.6	2.1	0.2	2.2	1.0	0.7	1.7	1.0	0.0	0.2	0.0	0.0	0.7	0.0	0.0	1.1	0.1	5.6
102	102, 116	1.6, 2.0	+0.7, +1.0	2.6	1.4	1.3	1.5	0.3	1.9	0.3	0.1	2.1	1.0	0.1	0.3	0.1	0.0	0.8	0.0	0.0	0.9	0.2	4.9
109	102, 116	2.4, 2.8	-1.0, -0.7	3.7	2.2	2.3	3.4	0.8	6.2	3.3	1.2	6.7	6.6	0.1	0.6	0.1	0.0	1.4	0.0	0.0	3.3	0.3	13.7
110	102, 116	2.4, 2.8	-0.7, -0.4	4.2	2.3	1.0	3.7	0.3	3.3	1.4	1.2	5.5	4.2	0.0	0.2	0.1	0.0	1.2	0.0	0.0	2.0	0.2	10.2
111	102, 116	2.4, 2.8	-0.4, 0.0	3.9	1.9	1.5	4.5	0.2	4.6	0.7	0.9	2.3	1.2	0.1	0.3	0.2	0.0	0.7	0.0	0.0	0.9	0.2	8.5
112	102, 116	2.4, 2.8	0.0, +0.4	3.1	1.5	0.7	2.9	0.1	3.2	0.6	0.4	2.3	1.3	0.1	0.3	0.1	0.0	0.8	0.0	0.0	0.9	0.1	6.3
113	102, 116	2.4, 2.8	+0.4, +0.7	2.7	1.6	1.1	1.7	0.2	1.6	1.2	0.8	4.0	2.1	0.0	0.2	0.1	0.0	1.2	0.0	0.0	1.4	0.2	6.5
114	102, 116	2.4, 2.8	+0.7, +1.0	2.2	1.4	1.3	1.5	0.3	2.4	2.0	0.8	3.3	3.2	0.1	0.6	0.1	0.0	1.3	0.0	0.0	2.2	0.1	7.0
127	116, 150	1.6, 2.0	-1.0, -0.7	8.4	1.7	8.7	7.1	2.9	29.0	0.2	0.4	1.8	1.2	0.0	0.1	0.0	0.0	0.6	0.0	0.0	0.7	0.2	32.5
128	116, 150	1.6, 2.0	-0.7, -0.4	7.6	2.0	4.2	9.0	1.3	8.6	0.6	0.2	0.3	0.5	0.0	0.1	0.0	0.0	0.6	0.0	0.0	0.5	0.2	15.4
129	116, 150	1.6, 2.0	-0.4, 0.0	-	-	-	-	-	-	-	-	-	-	-	-	-	-	-	-	-	-	-	
130	116, 150	1.6, 2.0	0.0, +0.4	-	-	-	-	-	-	-	-	-	-	-	-	-	-	-	-	-	-	-	
131	116, 150	1.6, 2.0	+0.4, +0.7	4.4	1.2	3.1	3.8	0.5	3.1	0.2	0.1	0.3	0.2	0.0	0.1	0.0	0.0	0.6	0.0	0.0	0.3	0.1	7.4
132	116, 150	1.6, 2.0	+0.7, +1.0	3.9	0.9	5.5	2.5	1.2	9.8	0.2	0.1	0.9	0.2	0.0	0.1	0.0	0.0	0.7	0.0	0.0	0.5	0.1	12.3
139	116, 150	2.4, 2.8	-1.0, -0.7	16.3	2.9	11.4	14.0	5.4	29.3	1.3	0.5	5.4	1.7	0.1	0.3	0.1	0.0	1.1	0.1	0.0	1.3	0.3	39.1
140	116, 150	2.4, 2.8	-0.7, -0.4	7.5	3.0	7.5	7.3	1.2	10.7	0.2	0.2	1.2	1.4	0.0	0.2	0.1	0.0	0.9	0.0	0.0	1.6	0.3	17.2
141	116, 150	2.4, 2.8	-0.4, 0.0	6.0	1.7	3.8	5.6	0.5	6.8	0.2	0.1	1.8	0.5	0.1	0.4	0.1	0.0	0.6	0.1	0.0	0.9	0.1	11.6
142	116, 150	2.4, 2.8	0.0, +0.4	4.5	1.4	3.1	3.2	0.5	3.4	0.1	0.5	0.8	0.2	0.1	0.4	0.1	0.0	0.6	0.0	0.0	0.5	0.1	7.4
143	116, 150	2.4, 2.8	+0.4, +0.7	3.8	1.4	2.4	2.4	0.4	3.3	0.3	0.3	0.9	0.7	0.0	0.2	0.1	0.0	1.0	0.0	0.0	0.9	0.1	6.5
144	116, 150	2.4, 2.8	+0.7, +1.0	3.3	1.0	1.7	2.0	0.7	3.8	0.7	0.2	1.8	0.6	0.1	0.3	0.1	0.0	1.1	0.0	0.0	0.2	0.1	6.3

Bin	$m_{\mu\mu}$ [GeV]	$ y_{\mu\mu} $	$\cos \theta^*$	$\delta_{\text{unc}}^{\text{stat}}$ [%]	$\delta_{\text{unc}}^{\text{sig}}$ [%]	$\delta_{\text{unc}}^{\text{bkg}}$ [%]	$\delta_{\text{cor}}^{\text{bkg}}$ [%]	$\delta_{\text{cor}}^{\text{mj}}$ [%]	$\delta_{\text{cor}}^{\text{scl}}$ [%]	$\delta_{\text{cor}}^{\text{sag}}$ [%]	$\delta_{\text{cor}}^{\text{res}}$ [%]	$\delta_{\text{cor}}^{\text{rec}}$ [%]	$\delta_{\text{cor}}^{\text{id}}$ [%]	$\delta_{\text{cor}}^{\text{trig}}$ [%]	$\delta_{\text{cor}}^{\text{kfac}}$ [%]	$\delta_{\text{cor}}^{\text{zpt}}$ [%]	$\delta_{\text{cor}}^{\text{pdf}}$ [%]	$\delta_{\text{tot}}$ [%]
1	46, 66	0.0, 0.2	-1.0, -0.7	5.4	2.0	2.1	1.5	0.5	0.2	0.5	0.6	0.3	0.3	0.7	0.0	0.5	0.3	6.6
2	46, 66	0.0, 0.2	-0.7, -0.4	1.8	0.7	1.1	1.2	0.0	0.0	0.1	0.1	0.2	0.2	0.5	0.2	0.3	0.2	2.7
3	46, 66	0.0, 0.2	-0.4, 0.0	1.5	0.6	0.8	0.9	0.5	0.0	0.1	0.0	0.5	0.4	0.0	0.2	0.4	0.2	2.3
4	46, 66	0.0, 0.2	0.0, +0.4	1.5	0.6	0.9	0.9	0.5	0.0	0.1	0.1	0.5	0.4	0.0	0.2	0.5	0.2	2.3
5	46, 66	0.0, 0.2	+0.4, +0.7	1.9	0.6	1.2	1.2	0.0	0.1	0.1	0.4	0.2	0.2	0.5	0.2	0.3	0.2	2.8
6	46, 66	0.0, 0.2	+0.7, +1.0	5.7	2.0	3.6	1.8	0.5	0.1	1.0	0.1	0.3	0.3	0.8	0.2	0.6	0.8	7.7
79	66, 80	0.2, 0.4	-1.0, -0.7	2.3	1.1	0.5	0.6	0.7	0.1	0.7	0.4	0.2	0.2	0.3	0.0	0.0	0.1	3.0
80	66, 80	0.2, 0.4	-0.7, -0.4	1.3	0.7	0.3	0.4	0.1	0.1	0.2	0.1	0.3	0.3	0.0	0.0	0.0	0.1	1.7
81	66, 80	0.2, 0.4	-0.4, 0.0	1.4	0.7	0.4	0.3	0.2	0.1	0.2	0.2	0.4	0.4	0.0	0.1	0.1	0.3	1.8
82	66, 80	0.2, 0.4	0.0, +0.4	1.4	0.7	0.3	0.3	0.2	0.1	0.1	0.2	0.4	0.4	0.1	0.1	0.1	0.2	1.8
83	66, 80	0.2, 0.4	+0.4, +0.7	1.4	0.7	0.4	0.4	0.1	0.1	0.2	0.2	0.3	0.3	0.0	0.1	0.1	0.1	1.8
84	66, 80	0.2, 0.4	+0.7, +1.0	2.2	1.1	0.4	0.6	0.8	0.2	0.7	0.1	0.2	0.2	0.3	0.0	0.0	0.3	3.0
157	80, 91	0.4, 0.6	-1.0, -0.7	0.4	0.2	0.0	0.0	0.0	0.1	1.0	0.1	0.3	0.3	0.0	0.0	0.0	0.1	1.4
158	80, 91	0.4, 0.6	-0.7, -0.4	0.4	0.2	0.0	0.0	0.0	0.2	0.6	0.1	0.4	0.4	0.1	0.0	0.0	0.0	1.1
159	80, 91	0.4, 0.6	-0.4, 0.0	0.3	0.1	0.0	0.0	0.0	0.2	0.3	0.1	0.3	0.3	0.0	0.0	0.0	0.0	0.9
160	80, 91	0.4, 0.6	0.0, +0.4	0.3	0.1	0.0	0.0	0.0	0.2	0.3	0.1	0.3	0.3	0.0	0.0	0.0	0.0	0.9
161	80, 91	0.4, 0.6	+0.4, +0.7	0.4	0.2	0.0	0.0	0.0	0.2	0.6	0.0	0.4	0.4	0.1	0.0	0.0	0.0	1.1
162	80, 91	0.4, 0.6	+0.7, +1.0	0.4	0.2	0.0	0.0	0.0	0.2	1.1	0.1	0.3	0.3	0.1	0.0	0.1	0.0	1.4
235	91, 102	0.6, 0.8	-1.0, -0.7	0.4	0.2	0.0	0.0	0.0	0.1	0.5	0.0	0.3	0.3	0.1	0.0	0.1	0.0	1.0
236	91, 102	0.6, 0.8	-0.7, -0.4	0.3	0.2	0.0	0.0	0.0	0.1	1.0	0.0	0.4	0.4	0.2	0.0	0.0	0.0	1.3
237	91, 102	0.6, 0.8	-0.4, 0.0	0.3	0.1	0.0	0.0	0.0	0.1	0.3	0.0	0.2	0.2	0.0	0.0	0.0	0.0	0.8
238	91, 102	0.6, 0.8	0.0, +0.4	0.3	0.1	0.0	0.0	0.0	0.2	0.3	0.0	0.3	0.2	0.0	0.0	0.0	0.0	0.8
239	91, 102	0.6, 0.8	+0.4, +0.7	0.3	0.2	0.0	0.0	0.0	0.2	1.0	0.0	0.4	0.4	0.1	0.0	0.0	0.0	1.3
240	91, 102	0.6, 0.8	+0.7, +1.0	0.4	0.2	0.0	0.0	0.0	0.1	0.5	0.0	0.3	0.3	0.1	0.0	0.1	0.1	1.0
313	102, 116	0.8, 1.0	-1.0, -0.7	2.1	1.0	0.1	0.4	0.0	0.2	0.9	1.4	0.4	0.4	0.2	0.0	0.0	0.1	3.0
314	102, 116	0.8, 1.0	-0.7, -0.4	1.8	0.8	0.0	0.2	0.1	0.2	1.8	0.3	0.3	0.2	0.0	0.0	0.0	0.0	2.8
315	102, 116	0.8, 1.0	-0.4, 0.0	1.7	0.7	0.0	0.1	0.0	0.1	0.4	0.6	0.3	0.3	0.1	0.0	0.0	0.0	2.0
316	102, 116	0.8, 1.0	0.0, +0.4	1.6	0.6	0.0	0.1	0.0	0.2	0.4	0.5	0.3	0.3	0.0	0.0	0.0	0.0	2.0
317	102, 116	0.8, 1.0	+0.4, +0.7	1.6	0.7	0.0	0.2	0.1	0.2	2.0	0.8	0.4	0.3	0.1	0.0	0.0	0.1	2.8
318	102, 116	0.8, 1.0	+0.7, +1.0	2.0	0.9	0.1	0.3	0.0	0.2	0.8	1.5	0.4	0.4	0.0	0.0	0.0	0.0	2.7
391	116, 150	1.0, 1.2	-1.0, -0.7	4.1	1.2	0.3	1.3	0.	0.1	0.5	0.3	0.5	0.5	0.2	0.1	0.0	0.1	4.8
392	116, 150	1.0, 1.2	-0.7, -0.4	2.9	0.7	0.2	0.7	0.1	0.1	0.7	0.4	0.4	0.3	0.2	0.0	0.1	0.1	3.4
393	116, 150	1.0, 1.2	-0.4, 0.0	2.5	0.6	0.1	0.5	0.1	0.1	0.5	0.1	0.3	0.3	0.2	0.0	0.1	0.1	2.8
394	116, 150	1.0, 1.2	0.0, +0.4	2.2	0.6	0.1	0.4	0.0	0.0	0.5	0.0	0.3	0.3	0.1	0.0	0.1	0.1	2.5
395	116, 150	1.0, 1.2	+0.4, +0.7	2.3	0.6	0.2	0.5	0.0	0.0	0.4	0.3	0.3	0.3	0.0	0.0	0.1	0.0	2.6
396	116, 150	1.0, 1.2	+0.7, +1.0	3.2	0.9	0.3	0.7	0.1	0.1	0.8	0.1	0.5	0.5	0.0	0.0	0.0	0.1	3.8
469	150, 200	1.2, 1.4	-1.0, -0.7	11.1	1.5	1.2	2.9	0.1	0.3	2.7	0.5	0.7	0.5	0.2	0.1	0.0	0.1	13.6
470	150, 200	1.2, 1.4	-0.7, -0.4	5.6	0.8	0.5	1.4	0.0	0.1	1.3	0.1	0.5	0.4	0.2	0.0	0.0	0.1	6.2
471	150, 200	1.2, 1.4	-0.4, 0.0	4.6	0.6	0.3	0.9	0.1	0.0	1.0	0.2	0.4	0.4	0.2	0.0	0.0	0.1	5.1
472	150, 200	1.2, 1.4	0.0, +0.4	4.1	0.5	0.2	0.7	0.1	0.0	1.1	0.0	0.4	0.4	0.1	0.0	0.0	0.0	4.5
473	150, 200	1.2, 1.4	+0.4, +0.7	4.0	0.5	0.2	0.8	0.0	0.1	0.8	0.2	0.4	0.4	0.0	0.0	0.0	0.1	4.3
474	150, 200	1.2, 1.4	+0.7, +1.0	6.6	0.9	0.5	1.2	0.1	0.0	1.7	0.0	0.6	0.5	0.0	0.0	0.1	0.1	8.0

3

# Appendix

$m_{\ell\ell}$ [GeV]	$d\sigma/dm_{\ell\ell}$ [pb/GeV]	$\delta^{\text{stat}}$ [%]	$\delta_{\text{unc}}^{\text{syst}}$ [%]	$\delta_{\text{cor}}^{\text{syst}}$ [%]	$\delta^{\text{total}}$ [%]
46, 66	$7.61 \times 10^{-1}$	0.2	0.1	0.9	0.9
66, 80	1.13	0.1	0.1	0.4	0.4
80, 91	21.4	0.0	0.0	0.2	0.2
91, 102	25.0	0.0	0.0	0.2	0.2
102, 116	$8.25 \times 10^{-1}$	0.2	0.1	0.4	0.4
116, 150	$1.64 \times 10^{-1}$	0.3	0.1	0.7	0.7
150, 200	$3.66 \times 10^{-2}$	0.5	0.2	1.3	1.4

# The ATLAS experiment

The diagram illustrates the ATLAS detector at the Large Hadron Collider (LHC). The detector is shown in a cutaway view, revealing its internal components. Labels identify several parts: Muon chambers, Toroid magnets, Solenoid magnet, Transition radiation tracker, Semiconductor tracker, Pixel detector, LAr electromagnetic calorimeters, LAr hadronic end-cap and forward calorimeters, and Tile calorimeters. A dimension line indicates a height of 25m from the base to the top of the muon chambers, and another line indicates a total length of 44m for the entire detector assembly. To the right, a smaller inset diagram shows two circular end-caps of the detector, each containing a complex network of lines and points representing particle trajectories. A coordinate system is overlaid on the inset, showing axes labeled  $\hat{p}_T$ ,  $\hat{p}_{\text{Parton}}$ , and  $\hat{p}_{\text{Parton}2}$ . Below the inset, a ground-level view shows the LHC ring as a white curve above a brown earth surface, with a small building and trees visible in the background.

LHC: proton synchrotron  
Circumference: 27km  
Center-of-mass energy: 13 TeV  
40 MHz collisions (1 kHz recorded)

Ulla Blumenschein, DIS 2018, Kobe

31

17/04/18